Cell. Mol. Life Sci. (2010) 67:1735–1750
DOI 10.1007/s00018-010-0280-3

Cellular and Molecular Life Sciences

RESEARCH ARTICLE

Lamellipodia mediate the heterogeneity of central olfactory ensheathing cell interactions

Louisa C. E. Windus · Katie E. Lineburg · Susan E. Scott · Christina Claxton · Alan Mackay-Sim · Brian Key · James A. St John

Received: 23 December 2009 / Revised: 14 January 2010 / Accepted: 19 January 2010 / Published online: 9 February 2010

Abstract The growth and guidance of primary olfactory axons are partly attributed to the presence of olfactory ensheathing cells (OECs). However, little is understood about the differences between the subpopulations of OECs and what regulates their interactions. We used OEC-axon assays and determined that axons respond differently to peripheral and central OECs. We then further purified OECs from anatomically distinct regions of the olfactory bulb. Cell behaviour assays revealed that OECs from the olfactory bulb were a functionally heterogeneous population with distinct differences which is consistent with their proposed roles in vivo. We found that the heterogeneity was regulated by motile lamellipodial waves along the shaft of the OECs and that inhibition of lamellipodial wave activity via Mek1 abolished the ability of the cells to distinguish between each other. These results demonstrate that OECs from the olfactory bulb are a heterogeneous population that use lamellipodial waves to regulate cell–cell recognition.

Keywords Olfactory bulb · Axon · Regeneration · Glia · Mek1

Introduction

The primary olfactory system is one of few regions within the mature vertebrate nervous system to exhibit continual turnover of neurons and a capacity for axon growth throughout life. Regenerating primary olfactory sensory neurons extend axons through a transitional zone between the peripheral and central nervous systems in order to reach their targets in the olfactory bulb. This regenerative capacity has been attributed to the presence of a specialized population of macroglia called olfactory ensheathing cells (OECs), which populate the peripheral olfactory nerve as well as the outermost layers of the olfactory bulb in the central nervous system [1–3]. OECs are thus believed to play a role in the establishment and maintenance of the olfactory nerve and in the sorting of axons within the nerve fibre layer (NFL) of the olfactory bulb [3–5].

OECs are often classified into two broad categories: peripheral OECs and central OECs. Peripheral OECs ensheathe the fascicles of mixed primary olfactory axons that project from the olfactory epithelium to the olfactory bulb, and are thought to be crucial for the growth, guidance and survival of olfactory axons as they extend towards the olfactory bulb [6]. En route to the bulb these fascicles penetrate the cribriform plate and enter the outer layer of the olfactory bulb, the NFL, which lies within the central nervous system. The primary olfactory axons then defasciculate from the mixed bundles of axons, sort out and refasciculate with axons that express the same odorant receptor [7]. In this way, axons that arise from neurons expressing the same odorant receptor fasciculate together

Electronic supplementary material The online version of this article (doi:10.1007/s00018-010-0280-3) contains supplementary material, which is available to authorized users.

L. C. E. Windus · K. E. Lineburg · S. E. Scott · A. Mackay-Sim · J. A. St John (✉)
National Centre for Adult Stem Cell Research,
Eskitis Institute for Cell and Molecular Therapies,
Griffith University, Nathan 4111, Brisbane, QLD, Australia
e-mail: j.stjohn@griffith.edu.au

L. C. E. Windus · C. Claxton · B. Key
School of Biomedical Sciences,
The University of Queensland,
Brisbane, QLD, Australia

and finally project to their target glomeruli. The central OECs populate the NFL and are believed to contribute to the complex sorting of axons within this layer [8]. However, the NFL is not a uniform structure but varies considerably with anatomical location. The rostral and ventral NFL is relatively thick with distinct inner and outer layers, whereas the NFL in the dorsal and caudal regions is thin and without the distinct layers observed in the rostral and ventral NFL.

Most of the defasciculation and sorting of axons occurs when the axons first enter the rostral and ventral NFL [8, 9]; axons in the dorsal and caudal NFL are largely already sorted and are projecting to their target glomeruli [10]. Further, the olfactory bulb develops in a rostral–caudal gradient with the rostral regions developing first. For example, P2 glomeruli which are located in the ventral and rostral halves of the olfactory bulb develop from E18 onwards [7, 11], whereas the M72 glomeruli which are located in the dorsal and caudal halves of the olfactory bulb develop from P3 onwards [12]. Thus, it would appear that OECs in the different anatomical locations would have different characteristics, but evidence to support this is currently lacking. We therefore hypothesized that the behaviour of cell–cell interactions of OECs from the NFL would vary depending on the anatomical location and developmental age, and that the behaviour of central OECs would differ to that of OECs in the peripheral olfactory nerve. We further hypothesized that the interactions would be regulated by lamellipodial waves that we have previously shown are crucial for regulating peripheral OEC interactions [13].

We examined the behaviour of cell–cell interactions of OECs from four different anatomical regions of the NFL and compared them to peripheral OECs throughout development. The behaviour of OECs within the NFL varied considerably depending on their anatomical location and the developmental age. We also found that the responses to cell–cell interactions were regulated via lamellipodial waves and that loss of wave activity reduced the ability of OECs to recognize and interact with each other. These results demonstrate that OECs are a functionally heterogeneous population of cells and that the resultant behaviours of OEC cell–cell interactions are consistent with their proposed roles in vivo.

Materials and methods

Generation of OMP-ZsGreen transgenic mice

Transgenic mice expressing ZsGreen in olfactory sensory neurons were generated. In these mice, the full-length (5.5-kb) olfactory marker protein (OMP) promoter [14] drove the expression of ZsGreen fluorescent protein, from pZsGreen-Express Vector (Clontech, Palo Alto, CA). OMP is selectively expressed at high levels in mature olfactory sensory neurons [15]. The transgene was liberated from the vector using EcoR1 restriction sites and injected into fertilized mouse oocytes at the Transgenic Animal Service of Queensland (University of Queensland, Brisbane). Successful integration of the transgene was confirmed by expression of ZsGreen fluorescence in the olfactory system of living neonatal animals. In these animals the vast majority of primary olfactory neurons express ZsGreen. The OMP-ZsGreen mice were then crossed with S100ß-DsRed transgenic mice that had been previously generated [13]. All procedures were carried out with the approval of, and in accordance with, the Griffith University Animal Ethics Committee and the Australian Commonwealth Office of the Gene Technology Regulator.

Immunohistochemistry

Adult S100ß-DsRed mice [13] were asphyxiated by CO_2 and their heads were fixed in 4% paraformaldehyde and sectioned (30 µm) on a cryostat microtome. Immunohistochemistry was performed as previously described [13] and sections were incubated with either polyclonal rabbit anti-p75NTR (1:500; Chemicon, Temecula, CA) or polyclonal rabbit anti-NPY (1:400; DakoCytomation, Glostrup, Denmark) or polyclonal rabbit anti-human S100ß (1:1,000; DakoCytomation), followed by goat anti-rabbit secondary antibodies conjugated to biotin (1:200; Vector Laboratories, Burlingame, CA) and then with streptavidin-conjugated Alexa Fluor^{488} (1:400; Molecular Probes, Carlsbad, CA).

Isolation of OECs from the lamina propria and olfactory bulb

Embryonic day 17 (E17) and postnatal day 2.5 (P2.5) S100ß-DsRed mice were killed by decapitation; adult mice were killed by CO_2 asphyxiation. Peripheral OECs were isolated from olfactory nerve fascicles within the lamina propria underlying the olfactory epithelium of the nasal septum using our previously published method [13]. Central OECs were prepared from the NFL of the olfactory bulbs. To obtain central OECs from the entire NFL, the olfactory bulb was removed from the cranial cavity and the NFL from the entire bulb was dissected. To obtain rostral, dorsal, caudal and ventral derived OECs, the NFL was directly taken from the corresponding anatomical regions (Fig. 4). The lamina propria and NFL tissue were incubated in plastic 24-well plates coated with Matrigel basement membrane matrix (10 mg/ml; BD Biosciences, San Jose, CA) and maintained in Dulbecco's modified

Eagle's medium containing 10% fetal bovine serum (E17 and P2 tissue) or 20% fetal bovine serum (adult tissue), G5 supplement (Gibco), gentamicin (Gibco, 50 mg/ml) and L-glutamine (200 μM) at 37°C in an atmosphere containing 5% CO_2 for 3–5 days (E17 and P2) or 2 weeks (adult). Contaminating macrophages were removed by incubation with TrypLE Express (Gibco) for 2 min. OECs were incubated with TrypLE Express for a further 4–5 min and then transferred to glass-bottomed 24-well plates coated with Matrigel and maintained in the same medium. All time-lapse images were acquired after 24–72 h from the first plating.

Growth factor and inhibitor assays of central OECs

OECs were incubated with each of the following: recombinant rat glial cell line-derived neurotrophic factor (GDNF; Bio-Scientific, NSW, Australia), nerve growth factor (NGF; Invitrogen Corporation, Melbourne, Australia) at final concentrations of 10 ng/ml and 20 ng/ml; JNK inhibitor II SP600125 (50 nM; Sigma-Aldrich), Src family kinase inhibitor PP2 (5 μM; Calbiochem, Merck, Darmstadt, Germany), the inactive analogue PP3 (5 μM; Calbiochem), Rac 1 inhibitor (NSC23766, 5, 10 μM; Calbiochem), and Mek 1 inhibitor (ethanolate U0126; 5, 10, 20 μM; Sigma–Aldrich).

Axon outgrowth assay

Monolayers of either central or peripheral derived OECs were plated on glass-bottomed 24-well plates coated with Matrigel and maintained for 8 h in the same medium as described above. Explants of olfactory neuroepithelium from E12-E14 OMP-ZsGreen mice were then plated directly onto the monolayer. The medium was changed and explants were then maintained in Neurobasal medium (GIBCO) supplemented with B27 (20 μl/ml), l-glutamine (4 μl/ml), 5 μl/ml of gentamicin at 1 mg/ml, HEPES (10 μl/ml at 10 mM) and *N*-methyl cellulose (100 μl/ml). Axon outgrowth occurred within 24 h. For the assay, six to eight explants were cultured per plate with ten plates in total, with embryos derived from 5 litters.

Time-lapse and fixed tissue imaging

Time-lapse images were routinely acquired at intervals of 15–30 s over periods of 40–60 min using an AxioCam MRm digital camera and a Uniblitz VCM01 shutter on an inverted Zeiss Axioobserver Z1 microscope fitted with epifluorescence and differential interference contrast optics. Images were acquired with a Zeiss LD PlanNeo-FLUAR 25/0.8 water iris and a LD PlanNeo-FLUAR 20/0.75 air iris. During imaging culture plates were maintained at 37°C in an incubator chamber under an atmosphere containing 5% CO_2. Images were compiled using Axiovision Rel 4.6.3 (Zeiss, Germany) and colour-balanced in Adobe Photoshop v 10.0 without further digital manipulation. Images of fixed tissue were acquired on a Zeiss AxioImager Z1 with an Axiocam MRm digital camera using Axiovision software (Zeiss, Germany) and a Zeiss EC Plan-NeoFLUAR 20/0.75 air iris and an EC Plan-NeoFLUAR 5/0.15 air iris or on an Olympus IX81 scanning confocal microscope, using Olympus Fluoview Ver 1.7b software (Olympus, Tokyo).

Quantification of wave processes and migration rates

Time-lapse image sequences of primary OEC cultures were acquired and analysed with Axiovision Rel 4.6.3 (Zeiss, Germany). The distance measurement tool was used to trace the rate and direction of waves on cell processes. The average journey rate was defined as the total distance individual waves travelled over the total recording time. The number of waves that occurred on cell processes was summed over the 1-h recording period. Waves were measured only when they were clearly distinguishable from the leading edge of both the process upon which it travelled and adjacent cells. The migration rate of any given cell was calculated by tracing the total distance travelled by the cell body over the total recording period, a measure obtained using the Axiovision distance measurement tool.

Statistical analyses

The time-consuming nature of the time-lapse assays necessitated the collection of sufficient *n* values over several weeks. Typically for each OEC preparation, four animals would be used to prepare the cultures which would then give rise to about ten time-lapse sequences. Therefore, an *n* value of 40 would be obtained from cells derived from approximately ten animals from 2 to 3 l. Statistical significance for the migration rate was tested using a Kruskal-Wallis test and Dunn's Multiple Comparison test for post-hoc analysis. Statistical significance for all other measurements was determined using either the chi-squared test or Fisher's exact test for two variables.

Results

OECs are a heterogeneous population of cells

In vivo, OECs display distinct roles in the olfactory neuraxis. In the peripheral nervous system OECs ensheathe and promote the growth of olfactory neuron axons in tightly fasciculated bundles as they exit the olfactory epithelium and

extend towards the olfactory bulb (Fig. 1a). In the central nervous system OECs reach the outer NFL (Fig. 1b, oNFL) and are intermingled with the axons as the axons undergo defasciculation and sorting out (Fig. 1a). In the inner NFL (Fig. 1b, iNFL) the OECs assist in the refasciculation of axons expressing the same odorant receptors (Fig. 1a).

Consistent with previous reports [5, 16, 17], we found that central and peripheral populations of OECs express different antigenic markers. Using coronal sections from adult S100ß-DsRed transgenic mice [13], we found that S100ß-DsRed is expressed by peripheral OECs in the olfactory nerve (Fig. 1d, e, ON) and by central OECs in both the oNFL and iNFL (Fig. 1b). Endogenous S100ß immunostaining (Fig. 1c, green fluorescence) was absent from the DsRed-positive iNFL (Fig. 1c). Since the distribution of endogenous S100ß varies across the depth of the NFL in different

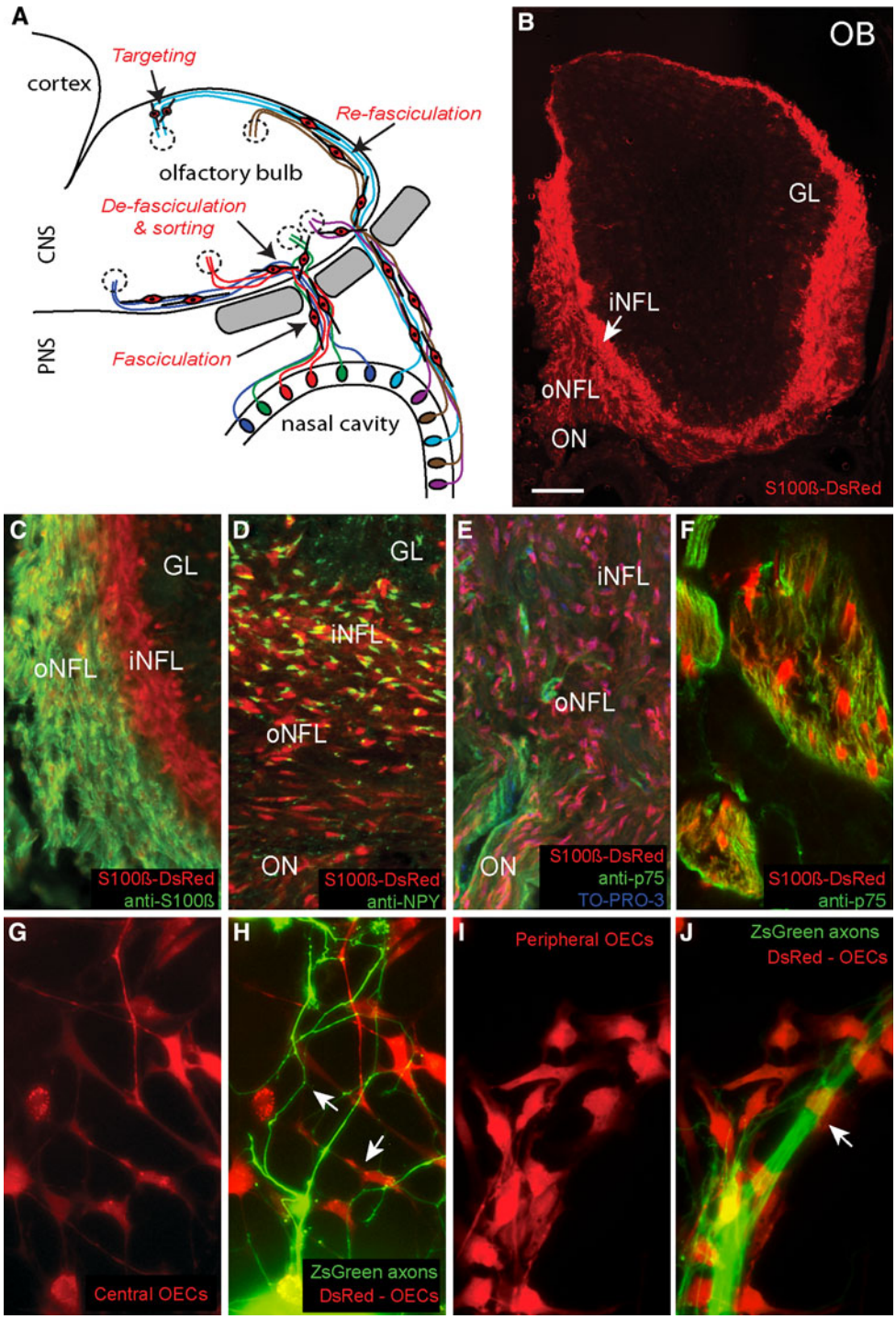

Fig. 1 OECs are a heterogeneous population. **a** Diagram depicting the olfactory system. In the peripheral nervous system, OECs ensheathe primary olfactory axons in tightly fasciculated bundles. Once they reach the central nervous system, OECs contribute to the defasciculation, sorting and refasciculation of the olfactory axons. **b–e** Coronal sections through the olfactory bulb and olfactory nerve with dorsal to the top and lateral to the right. **b** Low magnification of the olfactory bulb depicting OECs in the NFL of a S100ß-DsRed adult mouse. **c** A higher magnification view of the NFL. DsRed-expressing OECs (*red*) are present throughout the NFL, whereas S100ß detected by antibody staining (*green*) is present in the oNFL. **d** The OECs of the iNFL express neuropeptide Y, whereas OECs in the oNFL do not. **e** p75ntr is clearly expressed by OECs present in the peripheral olfactory nerve (*ON*) and sparsely throughout the oNFL. **f** Section through the lamina propria shows that peripheral OECs express both DsRed and p75NTR. **g–j** Primary olfactory axons in vitro grown on monolayers of either central (**g**) or peripheral (**i**) derived OECs. When plated on central OECs, axons are spatially dispersed (**h**, *arrows*) while axons grown on peripheral OECs are closely associated (**j**, *arrow*). *CNS* central nervous system, *PNS* peripheral nervous system, *GL* glomerular layer, *OE* olfactory bulb, *ON* olfactory nerve. *Scale bars* **b** 300 µm, **c–e** 75 µm, **f–j** 35 µm

species [8, 18, 19], it was fortuitous that the human S100ß regulatory sequences used to drive expression of DsRed produced ubiquitous expression in OECs of the NFL. OECs in the iNFL were positive for neuropeptide Y (Fig. 1d) but lacked the low-affinity neurotrophin receptor p75NTR (Fig. 1e). Anti-p75NTR immunostaining was present on peripheral OECs throughout the olfactory nerve (Fig. 1e, f).

While it is clear that peripheral and central OECs have different roles and antigenic profiles in vivo [20–24], there are no experimental data to support a clear antigenic or functional distinction between theses two spatially different sources of OECs in vitro [25–27]. In fact peripheral and central OECs have remarkable similarities in vitro including similar phenotypes and molecular markers [28]. However, we know little of how at the cellular level OECs interact with themselves or other cell types in vitro. Using high-resolution time-lapse microscopy we endeavoured to investigate whether there were differences in how central or peripheral derived OECs interacted with themselves or olfactory axons in vitro.

In order to selectively identify and visualize peripheral OECs derived from the lamina propria and central OECs derived from the olfactory bulb for time-lapse studies, we cultured cells from S100ß-DsRed transgenic mice [13] and maintained the cells in culture for one passage only. In culture there were striking differences between the two populations of OECs. Central OECs were spatially dispersed (Fig. 1g) with a small proportion of cells in direct contact with each other. In contrast, peripheral OECs were highly adherent with the majority of cells in close contact with each other (Fig. 1i). We next grew primary olfactory neurons cultured from the neuroepithelium of the OMP-ZsGreen transgenic line. When grown on a monolayer of central OECs, axons were consistently spatially dispersed (Fig. 1h) in comparison to axons grown on peripheral OECs which were in close proximity to each other and more resembled a fasciculated phenotype (Fig. 1j). It was clear that olfactory axons migrated directly along the processes and cell body of OECs using them as preordained migratory pathways (Fig. 1h, j, arrows) and that the distribution of axons was determined primarily by the spatial orientation of the OECs. We therefore wanted to further investigate what mechanisms mediate these fundamental differences in OEC cellular behaviour as it appeared that the differing interactions of the OECs influenced the spatial organization of the outgrowing axons.

Peripheral and central OECs respond differently to cell–cell contact

The more dispersed nature of the central OECs in vitro suggested that there could be differences in adhesion/repulsion between cells. We therefore tested whether subpopulations of OECs display differential cellular responses during cell–cell contact using in vitro assays that we had previously established [13]. In these assays, primary cultures of OECs were replated at densities that allowed high-resolution time-lapse microscopy of cells as they were undergoing initial cell–cell contact and interactions.

We first examined the behaviour of peripheral OECs derived from E17, P2 or adult tissue. We consistently found that when two peripheral OECs initiated cell–cell contact, the interaction overwhelmingly led to adhesion (data not shown, but interaction is similar to that shown for central OECs in Fig. 2a). In the context of these time-lapse analyses, adhesion was defined as both processes remaining in contact with each other for at least 1 h, which was the limit of our imaging sequences. This adhesive behaviour was consistent regardless of the age of the donor tissue (86–90% of interactions, Fig. 2d).

We next investigated OECs derived from the entire NFL of the olfactory bulb. To obtain these cells, the NFL from all regions of the olfactory bulb was cultured together with cells from the rostral, ventral, dorsal and caudal regions (see Fig. 4a). The behaviour of central OECs was remarkably different from that of peripheral OECs. When two central OECs initiated cell–cell contact, the interaction resulted in a mix of behaviour including adhesion (Fig. 2a), repulsion (Fig. 2b) and continuing to grow over each other without exhibiting any adhesion or repulsion (crossover, Fig. 2c). During adhesive interactions, the leading edge of one OEC (Fig. 2a, arrow) would contact the shaft of another OEC (Fig. 2a, asterisk). The two processes would actively interact with each other (Fig. 2a, 04.17–9.27, arrows, arrowheads) which resulted in fusion of two OEC processes (Fig. 2a, 45.16, asterisk; Supplementary material 1). Typically during repulsive interactions, the leading edge of an OEC process (Fig. 2b, arrow) would approach the shaft of another OEC (Fig. 2b, asterisk), make initial contact (Fig. 2b, 16.42, arrow) but then actively withdraw from the shaft (Fig. 2b, 33.42, arrow) while the other cell also displayed a retraction response; after retraction the cells would make no further contact (Supplementary material 2). Typically during a crossover interaction, two OEC processes would interact with each other (Fig. 2c, arrowhead), but the processes would continue to extend along different paths without adhering to or repelling each other. Despite having ongoing opportunities to interact via small lamellipodial waves, neither of the cells appeared to respond (Fig. 2c, 06.40–40.00; Supplementary material 3).

When derived from embryonic tissue, cell–cell contact of central OECs resulted in an equal mix of adhesion (32%), repulsion (38%) and continuing to grow to cross over each other without exhibiting any adhesion or repulsion (crossover, 30%; Fig. 2e).

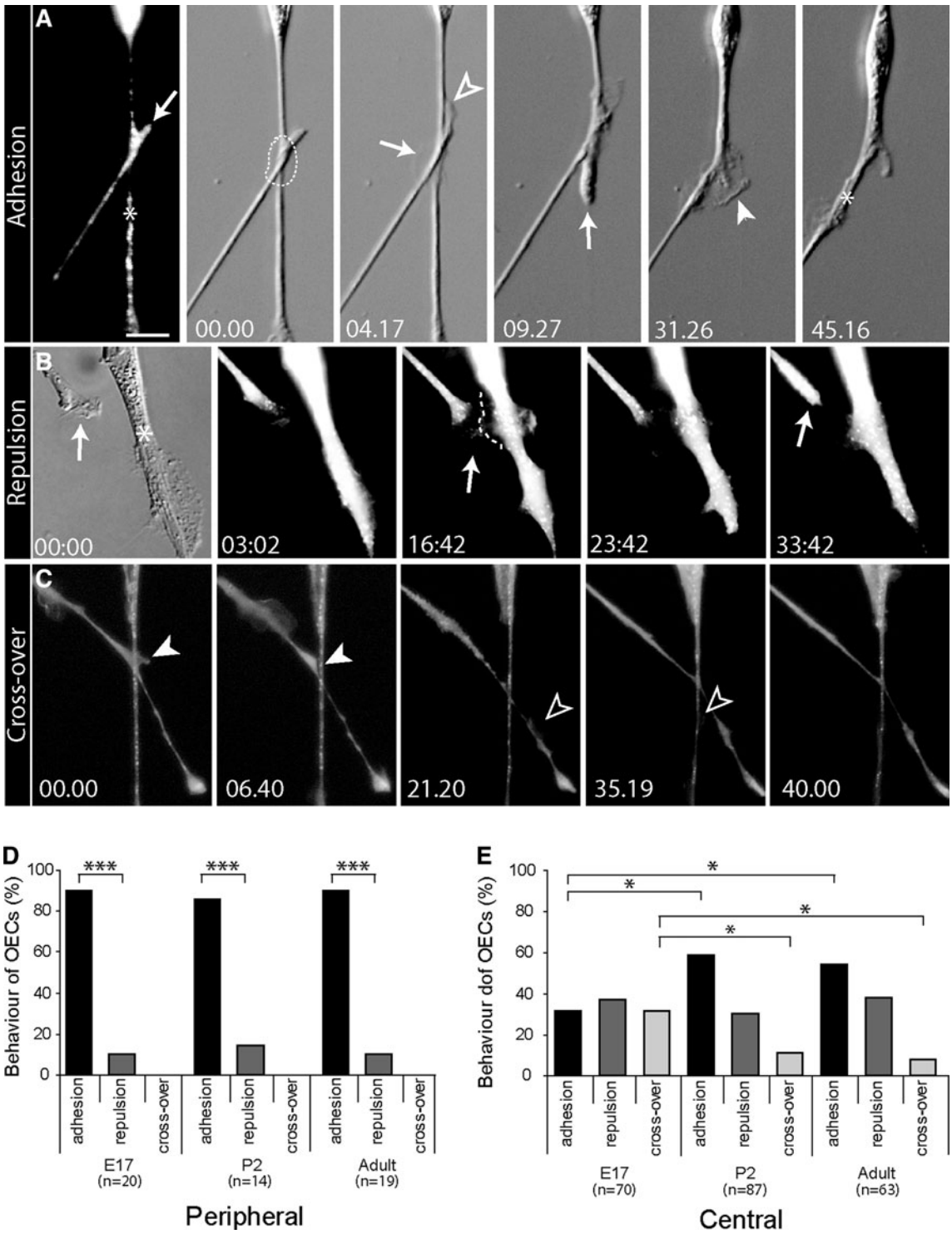

Interestingly, when derived from postnatal or adult mice, central OECs had increased adhesion responses (58% P2, 54% adult; Fig. 2e) but maintained their repulsion responses. Thus, the increase in adhesion responses was at the expense of crossover responses. However, the responses of central OECs regardless of age were different from the responses of peripheral OECs, which always overwhelmingly showed adhesion (Fig. 2d).

These results suggest that:

1. Peripheral OECs derived from tissue of all ages consist of a homogeneous population of cells that primarily adhere to one another during cell–cell contact.

◀ **Fig. 2** OEC cell–cell interactions in vitro result in a mix of responses. Centrally derived OECs display three specific behaviours (**a–c**) during cell–cell interaction in vitro. **a** *Adhesion*: expression of S100ß-DsRed identifies two interacting OECs. The leading edge (*arrow*) is in contact with the shaft (*asterisk*) of a second OEC. Time-lapse differential interference contrast (DIC) images reveal that a lamellipodial wave is present at the point of contact (00.00, *dotted line*; 04.17, *arrow*) between the two processes. The leading edge interacts with the lamellipodial wave and then proceeds to align and adhere to the shaft of the second process (04.17, *unfilled arrowhead*). The shaft of the second OEC then retracts (09.27, *arrow*). The lamellipodial wave and leading edge actively interact (16.57, *arrowhead*) resulting in adhesion between the two OECs (45.16, *asterisk*). Sequences are taken from Supplementary material 1. **b** *Repulsion*: DIC image reveals an active leading edge of a central OEC (*arrow*) migrating towards the shaft of a second OEC process (*asterisk*). A lamellipodial wave emerges (*dotted line*) and briefly interacts with the leading edge (16.42, *arrow*) before the leading edge retracts (33.42, *arrow*). Sequences are taken from Supplementary material 2. **c** *Crossover*, whereby two OECs grow over each other without perturbation. A wave (*arrowhead*) present on a DsRed-positive OEC makes contact with the shaft of a second DsRed-positive OEC. Following contact with the second cell, the wave collapses (06.40, *arrowhead*). Further along the shaft a second wave emerges (21.20, *unfilled arrowhead*), travelling in a retrograde direction and contacting the shaft of the second OEC which again results in collapse (35.19, *arrow*) of the lamellipodial wave. The OEC continues to grow over the second OEC without any adherent or repellent activity (40.00). Sequences are taken from Supplementary material 3. The times indicated are in minutes and seconds. *Scale bar* 20 µm. **d** Peripheral OECs derived from embryonic, postnatal or adult tissue overwhelmingly display adhesion events; $p < 0.001$ chi-squared test, $^{***}p < 0.0015$ post-hoc Fisher's exact test. **e** Cell–cell contact of central OECs derived from embryonic tissue results in an even mix of adhesion, repulsion and crossover events when, but the behaviour of OECs derived from postnatal or adult tissue is significantly different; $p < 0.05$ chi-squared test, $^{*}p < 0.05$ post-hoc Fisher's exact test

2. Central OECs consist of a functionally heterogeneous population of cells that exhibit a mix of three distinct behaviours: adhesion, repulsion or crossover.

Central OECs display dynamic lamellipodial waves

We have previously shown that novel lamellipodial protrusions, termed lamellipodial waves, exist on the shafts of peripherally derived OECs and are crucial for mediating cell–cell contact and migration [13]. During the cell–cell contact assays with the central OECs (Fig. 2a–c), it was apparent that lamellipodial waves were often at the point of contact between the cells (e.g. Fig. 2a, dashed circle; Fig. 2b, dashed line; Fig. 2c, arrowhead). We therefore wanted to further investigate the occurrence and function of the lamellipodial waves on centrally derived OECs. Consistent with our previous work, we found that the dynamic lamellipodia were present along the shaft and/or cell body of central OECs (Fig. 3a) and that these lamellipodial waves were distinct from the leading edge (Fig. 3a, asterisk). The waves were not constantly present, but rather periodically appeared along the OEC shaft (Fig. 3a, 00:46:22, dashed line) and travelled in both retrograde (Fig. 3a, 00.02.21–00.24.41, arrowheads) and anterograde (Fig. 3a, 00.46.22–00.53.26, unfilled arrowhead) directions. Moreover, these waves were found to rapidly and dynamically move along the shaft in opposing directions (Fig. 3a, 00.53.26, anterograde wave, unfilled arrowhead; retrograde wave, dashed line) and would merge on the OEC process (Fig. 3a, 01.04.26, arrow; Supplementary material 4).

Lamellipodial waves initiate cell–cell contact

We have previously observed that when peripheral OECs interact with each other, lamellipodial waves mediate most of the initial direct cell–cell contacts, and that without lamellipodial waves cell–cell adhesion does not occur [13]. We have now examined central and peripheral OECs to determine the effect of the age of the tissue on the behaviour of lamellipodial waves and the resultant cell response.

During interactions of central OECs, lamellipodial waves were involved in 70–80% of all initial cell–cell interactions regardless of the age of the donor tissue, with all three cell–cell contact responses being observed: adhesion, repulsion and crossover. For those interactions in which waves were not present, the leading edge of an OEC directly contacted the shaft of another cell and no waves were generated at the point of contact. For E17 central OECs, there was an equal distribution of adhesion (38%), repulsion (26%) and crossover events (36%) (Fig. 3b). During adhesive interactions, a lamellipodial wave was often seen at the point of interaction between the leading edge of one OEC and the shaft of another (Fig. 2a, 00.00, dashed line; 04.17, arrow). The lamellipodial wave actively interacted with and engulfed the leading edge resulting in fusion of the two OEC processes (Fig. 2a, 45.16, asterisk). It is worth noting that for all adhesion events for E17-derived central OECs lamellipodial waves were always present at the site of contact (100%, $n = 21$ out of 21 interactions). During repulsive interactions, the wave was seen to first expand towards the incoming leading edge (Fig. 2b, 16.42, leading edge, arrow; wave, dashed line) and then rapidly reduce in size as the leading edge retracted (Fig. 2b, 33.42, arrow). During crossover events, a leading edge would briefly explore the lamellipodial wave before continuing directly over the process without adhering or repelling. In some instances, after the leading edge had crossed over the process, lamellipodial waves continued to survey the point of contact between the two processes (Fig. 2c, 00.00, arrowhead).

Wave-based interactions of central OECs from older animals resulted in increased adhesion (P2 68%; adult

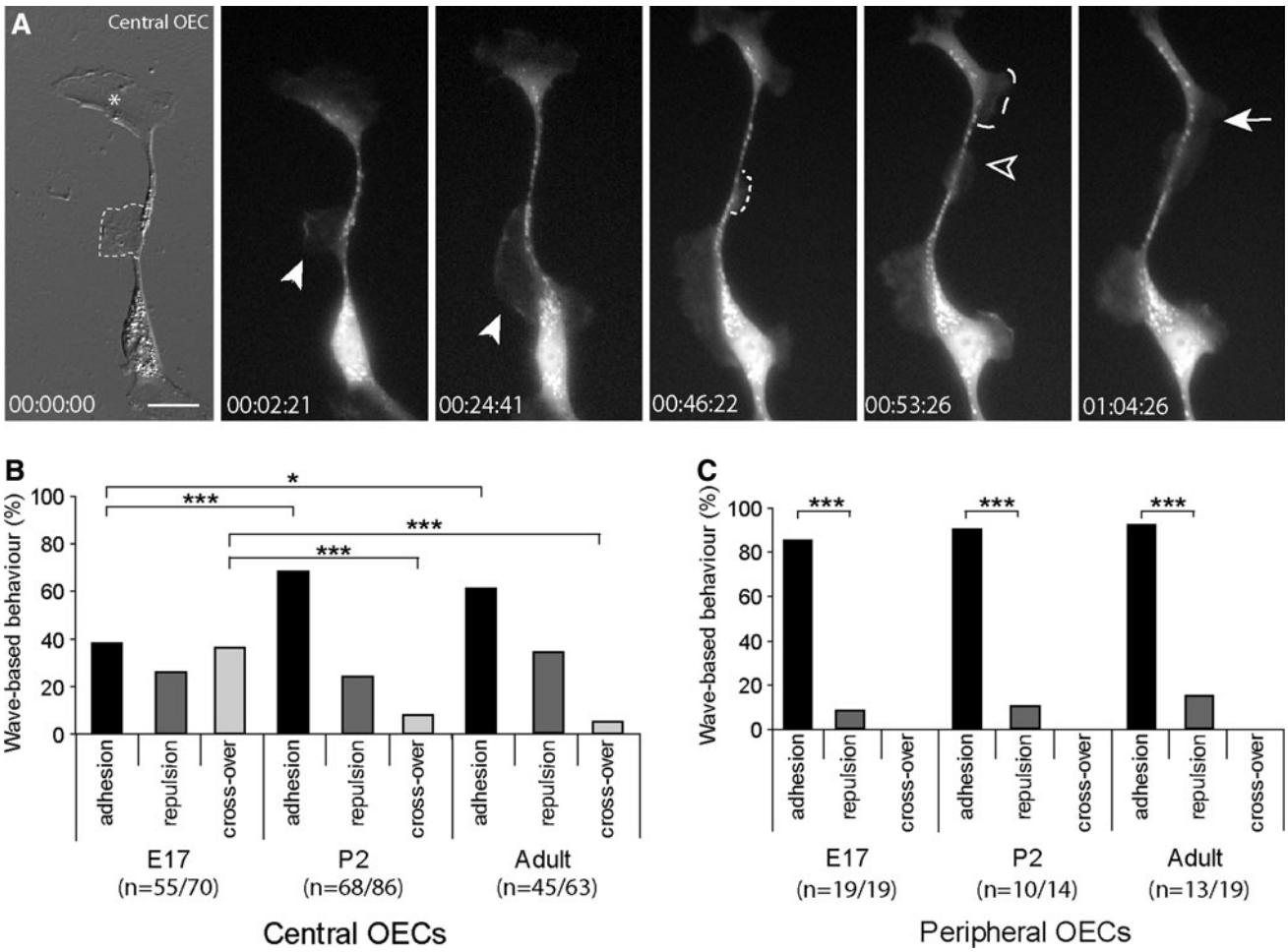

Fig. 3 Anterograde and retrograde travel of lamellipodial waves on an isolated central DsRed-expressing OECs in vitro. **a** DIC image reveals a single lamellipodial wave (*dashed line*) present on the shaft of the process that is distinct from the leading edge (*asterisk*). The cell strongly expressed DsRed fluorescence and subsequent time-lapse imaging reveals that several lamellipodial waves formed along the shaft. A single lamellipodial wave forms on the shaft and moves in a retrograde direction (00.02.21–00.24.41, *arrowhead*). A second wave forms (00.46.22, *dashed line*) and moves in an anterograde direction (00.53.26, *unfilled arrowhead*) toward a third lamellipodial wave (00.53.26, *dashed line*), and the waves merge (01.04.26, *arrow*) to form a single lamellipodial wave. Sequences are taken from Supplementary material 4. The times indicated are in hours, minutes and seconds. *Scale bar* 20 μm. **b**, **c** Resultant cellular behaviour following initial cell–cell contact when a lamellipodial wave was present at the site of contact was quantified for central OECs (**b**) and peripheral OECs (**c**); $p < 0.001$ chi-squared test, $^{*}p < 0.05$, $^{***}p < 0.001$ post-hoc Fisher's exact test

61%; Fig. 3b). However, one-quarter to one-third of interactions resulted in repulsion, and crossover events continued to be observed, although they constituted less than 10% of responses. Thus, wave-based interactions on central OECs continued to result in a mix of cell responses. More importantly, lamellipodial waves were consistently involved in initiating cell–cell contact during all behaviours including adhesion, repulsion and even crossover events (Fig. 3b).

For peripheral OECs derived from E17, P2 or adult tissue, the overwhelming majority of lamellipodial wave interactions resulted in cell–cell adhesion (Fig. 3c). Interestingly, all initial cell–cell contact events in OECs derived from E17 tissue occurred only in the presence of waves. For example, when the leading edge of one OEC approached a neighbouring OEC it would very selectively contact a lamellipodial wave on the other cell; it would never contact the shaft directly if a wave was not present (data not shown, but similar to that shown for central OECs in Fig. 2a). However, in OECs derived from older animals, lamellipodial waves were not always involved in initial cell–cell contact although they were still involved in about 70% of interactions with the majority of these interactions resulting in stable adhesive contacts (Fig. 3c). It should be noted that repulsion events did occur regardless of the age of the tissue; however, only around 10% of processes were found to display this behaviour, and crossover events were never observed (Fig. 2d). These results suggest that

lamellipodial waves are mechanisms for maintaining the intrinsic adhesive behaviour of peripheral OECs throughout development.

In summary, these results suggest that peripheral and central OECs show have intrinsically different behaviour following cell–cell contact and there is a clear bias for lamellipodial waves to initiate contact between OECs. In embryonic animals lamellipodial waves were always involved in mediating adhesion of OECs.

Subpopulations of central OECs respond differently to cell–cell contact

The development of the central region of the olfactory system is not uniform. At E11 the very rostral region of the presumptive NFL of the murine olfactory bulb is the first to develop. Nascent glomeruli become evident at E17 (Fig. 4a, d) and they develop across a gradient from rostral to caudal with this pattern continuing in the postnatal animal (Fig. 4b) with the established glomeruli being evident throughout the olfactory bulb in the adult (Fig. 4c). Moreover, the transition zone between the peripheral and central olfactory system lies in the rostral and ventral regions of the olfactory bulb (Fig. 4a, arrowheads) where axons primarily defasciculate and sort out, especially during embryonic and early postnatal development. The NFL in the ventral region is much thicker and glomeruli are larger (Fig. 4d, f, h) compared to the dorsal and caudal regions where the NFL is much thinner and glomeruli develop later (Fig. 4e, g, i). Based on these differences in anatomical development, we hypothesized that OECs cultured from distinct topographical locations of the olfactory bulb may also exhibit behaviourally different responses to cell–cell contact. Further, we rationalized that these differences would vary across different developmental stages. To investigate this, central OECs were dissected from rostral, dorsal, ventral and caudal regions of the NFL derived from E17, P2 or adult animals. Figure 4j shows an example of the careful dissection of the NFL to obtain the OECs from the dorsal and caudal regions.

We first examined OECs from the rostral NFL. Cells derived from E17 tissue predominantly showed repulsion events (60% of interactions, Fig. 4k), cells derived from P2 tissue showed more of a mix of adhesion (45%), repulsion (35%) and crossover events (20%) (Fig. 4k), and cells derived from adult tissue showed an even mix of adhesion, repulsion and crossover events. We can infer from these results that rostral OECs consistently display a mix of the three distinct behaviours throughout development.

We next examined OECs from the dorsal NFL. Cells derived from embryonic animals showed an equal mix of adhesion (35%), repulsion (35%) and crossover (30%) (Fig. 4l). Interestingly, cells derived from P2 and adult tissue showed an increase in adhesion events (57% in P2 cells, 56% in adult cells) but a significant decrease in crossover events (8% in P2 cells, 0% in adult cells). However, repulsion events remained constant across all developmental stages.

Similar results were found for OECs from the ventral NFL. Embryonic cells displayed a mix of adhesion (25%), repulsion (25%) and crossover events (50%) (Fig. 4m). However, postnatal and adult cells showed an increase in adhesion events (60% in P2 cells, 45% in adult cells), but a decrease in cross-over events (Fig. 4m).

Similar to dorsal and ventral OECs, caudal OECs derived from embryonic tissue exhibited an equal mix of adhesion (33%), repulsion (33%) and cross-over events (33%) (Fig. 4n). However, OECs derived from postnatal and adult tissue predominantly showed adhesion events (71% and 83%, respectively). Thus, caudal OECs derived from postnatal and adult tissue exhibited a more homogeneous response, and were similar to OECs derived from peripheral olfactory nerve.

These results clearly demonstrate that OECs from different regions of the NFL display distinct behavioural differences. Of particular note, OECs from the rostral NFL exhibited an equal mix of behaviours into adulthood whereas OECs from the caudal NFL displayed predominantly adhesion events. As lamellipodial waves were involved in the cell–cell contacts, we next investigated whether lamellipodial waves were crucial mechanisms in establishing cell–cell contact behaviour by modulating their behaviour independently of the leading edge.

GDNF regulates wave activity but does not change behaviour of central OECs

GDNF has been shown to mediate migration of OECs by binding to GFRα-1 and Ret and subsequently activating JNK and SRC kinases [29]. Previously we have reported that the generation of lamellipodial waves on peripheral OECs influences their migration rate, and the activity of these waves can be modulated by GDNF [13]. We examined the role of GDNF on centrally derived OEC migration and wave formation in the presence of exogenous GDNF.

Consistent with our previous results, the addition of GDNF to central OEC cultures derived from adult animals increased the rate of OEC migration fourfold (Fig. 5a). Inhibition of GDNF-based signalling with selective inhibitors of either JNK [30] or SRC [31] decreased OEC migration twofold (Fig. 5a). These results confirmed that GDNF is an important regulator of central OEC migration. It was also clear that GDNF had an effect on lamellipodial wave activity. Following the the addition of 10–20 ng/ml of GDNF, the number and size of waves exhibited by central OECs significantly increased. In the presence of

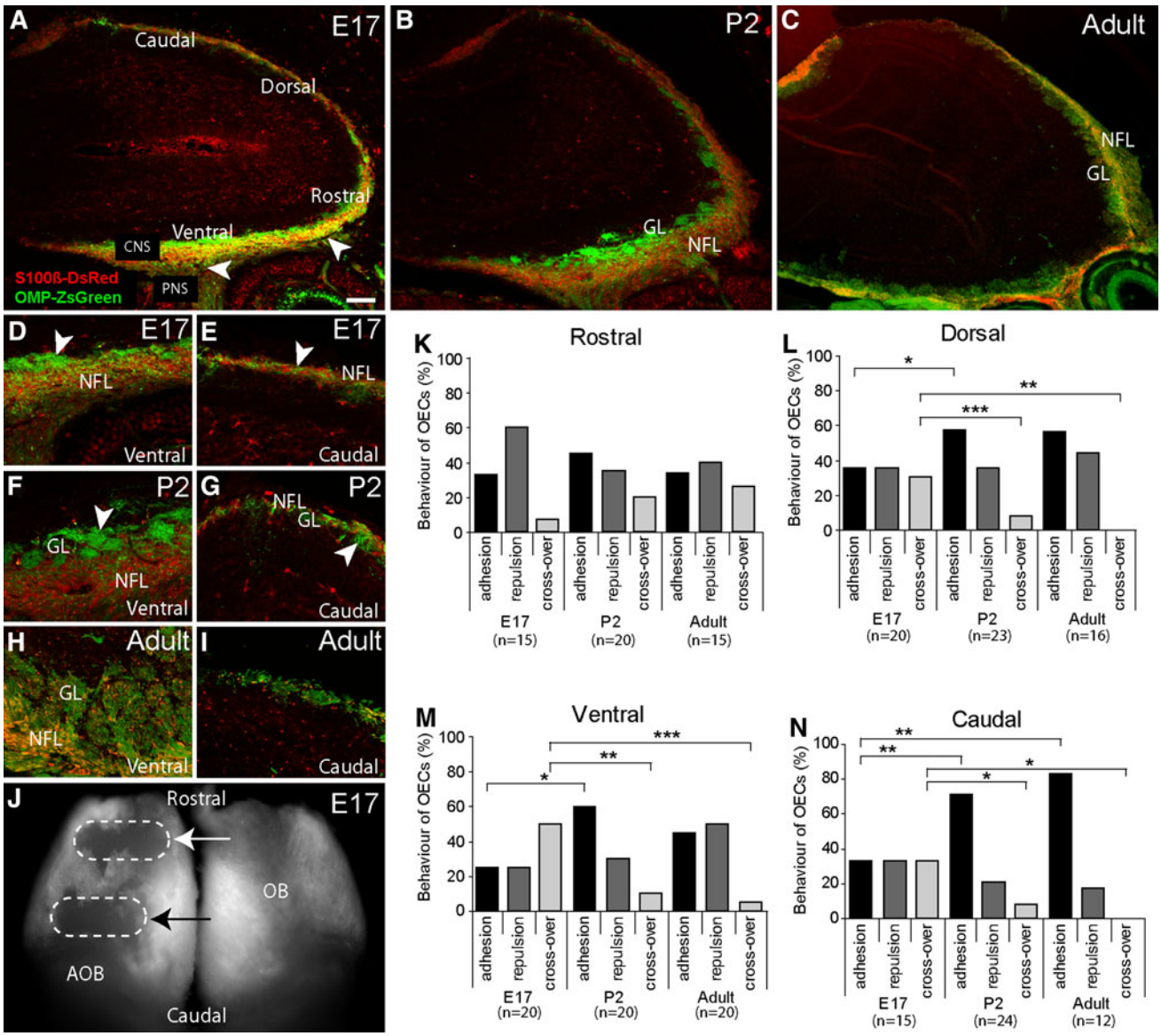

Fig. 4 The olfactory bulb develops in a distinct rostral to caudal gradient. In OMP-ZsGreen × S100ß-DsRed mice, primary olfactory axons (*green*) and OECs (*red*) are clearly visible. Parasagittal sections are shown with rostral to the right and dorsal to the top. **a** At E17 the olfactory bulb displays a distinct bulbar shape with a partial laminar organisation of the NFL. The transition zone (*arrowheads*) between the peripheral and central nervous systems occurs in the ventral and rostral region of the olfactory bulb. **b** At P2 there is a distinct increase in NFL organization with a distinguishable NFL and glomerular layer (*GL*) with glomeruli particularly visible in the rostral and ventral region of the olfactory bulb. **c** In adult mice, the ventral region of the olfactory bulb is thickly populated with well-formed glomeruli. **d**–**i** Higher magnification views of ventral and caudal regions of the NFL but from different sections to those in **a**–**c**. **d**, **e** At E17 the nascent glomeruli are detectable in the ventral NFL (**d**), but not in the caudal NFL (**e**). **f**, **g** At P2, the ventral region (**f**) has developed a band of glomeruli (*arrowhead*), while in the caudal region a thinly populated region of nascent glomeruli has formed (**g**, *arrowhead*). **h**, **i** In the adult, large glomeruli have formed (**h**) while the caudal region remains thinly populated (**i**). **j** OECs were dissected from the different regions of the olfactory bulb. The dissected areas are shown in a dorsal view of E17 olfactory bulbs of an OMP-ZsGreen mouse; rostral is to the top and caudal to the bottom. *Regions outlined by dashes* in the left olfactory bulb show the areas where OECs were obtained from the dorsal NFL (*white arrow*) and the caudal NFL (*black arrow*). The right olfactory bulb has not been dissected (*AOB* accessory olfactory bulb). Central OECs from different topographical areas have dissimilar responses to cell–cell contact in vitro. **k**–**n** Resultant behaviour of interacting central OECs derived from the rostral (**k**), dorsal (**l**), ventral (**m**) and caudal (**n**) olfactory bulb tissue; $p < 0.001$ chi-squared test, $^{*}p < 0.05$, $^{**}p < 0.01$, $^{***}p < 0.001$ post-hoc Fisher's exact test. *Scale bars* **a**–**c** 100 µm, **d**–**i** 30 µm , **j** 200 µm

GDNF, around 80% of central OECs subsequently displayed waves (Fig. 5b). The selective action of GDNF was evident since NGF, which is also expressed by OECs [32], did not elicit the same response (Fig. 5b). GDNF also increased the surface area of lamellipodial waves (Fig. 5c, d).

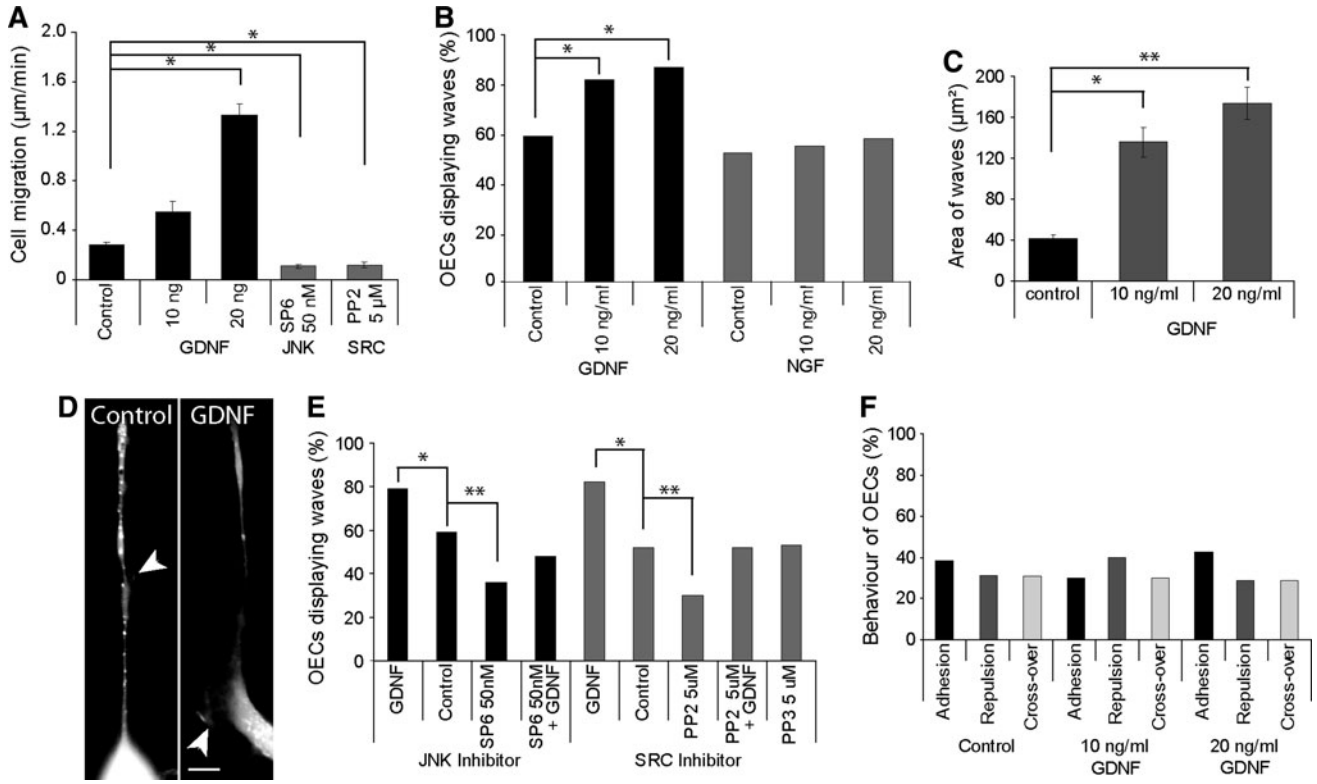

Fig. 5 GDNF influences central OEC cell migration and wave activity. OECs were obtained from the NFL of adult animals. **a** Central OECs migrate at higher rates following the addition of 20 ng/ml of GDNF; the addition of JNK (9SP600125) or SRC (PP2) inhibitors decreased migration of OECs (n=11–20); $p < 0.05$ Kruskal-Wallis test, $^{*}p < 0.05$ post-hoc Dunn's multiple comparison test. **b** Percentage of cells with lamellipodial waves following the addition of GDNF and NGF ($n = 11$–20); $p < 0.05$ chi-squared test, $^{*}p < 0.05$ post-hoc Fisher's exact test. **c** Quantification of the surface area of lamellipodial waves on isolated OECs following the addition of GDNF ($n = 11$–20); $p < 0.01$ Kruskal-Wallis test, $^{*}p < 0.05$, $^{**}p < 0.01$ post-hoc Dunn's multiple comparison test; *error bars* standard error of the mean. **d** Addition of GDNF dramatically increased the size of lamellipodial waves on OECs; *scale bar* 10 μm. **e** Inhibition of JNK (by SP600125) or SRC (by PP2) alone reduced the occurrence of lamellipodial waves; whereas addition of GDNF alone increased the occurrence of waves. When inhibitors were added together with GDNF the phenotype was rescued. Incubation with the inactive analogue PP3 had no effect on wave frequency compared to controls ($n = 11$–22) for all treatments; $p < 0.01$ chi-squared test, $^{*}p < 0.05$, $^{**}p < 0.01$ post-hoc Fisher's exact test. **f** The addition of GDNF did not alter the mix of behaviours of interacting OECs ($n = 7$–15; $p > 0.05$)

Since GDNF signalling involves both JNK and SRC, we next tested whether inhibition of these kinases would affect the behaviour of lamellipodial waves on central OECs. When OECs were incubated with the JNK inhibitor SP600125 or with the SRC inhibitor PP2, the percentage of OECs displaying lamellipodial waves was significantly reduced (Fig. 5e) whereas incubation with the inactive analogue PP3 had no effect. When central OECs were incubated with both GDNF (20 ng/ml) together with either SP600125 or PP2, the frequency of lamellipodial waves was reduced to control levels (Fig. 5e). The rescue of the phenotype by GDNF indicates that these kinases are acting downstream of this growth factor in central OECs.

We have reported here that lamellipodial waves are important mechanisms that mediate cell–cell contact between central OECs. We next tested whether addition of GDNF would affect the intrinsic behaviour of central OECs during cell–cell contact. OECs from the rostral region of the adult olfactory bulb continually displayed an equal mix of responses including adhesion, repulsion and crossover (Figs. 2a–c, 4k). With the addition of exogenous GDNF the resultant behaviour of interacting rostral OECs remained constant (Fig. 5f). The exogenous addition of GDNF at a concentration of either 10 ng/ml or 20 ng/ml did not disrupt or affect the intrinsic cell behaviour of interacting rostral OECs (Fig 5f). Hence increasing the activity of waves via GDNF does not alter the cell response.

Mek mediates lamellipodial wave formation and intrinsic cellular behaviour

We have previously reported that the activity of lamellipodial waves is regulated independently of the leading edge via the Mek intracellular pathway [13]. We next investigated whether lamellipodial waves on rostral OECs were regulated by similar intracellular signalling molecules. Consistent

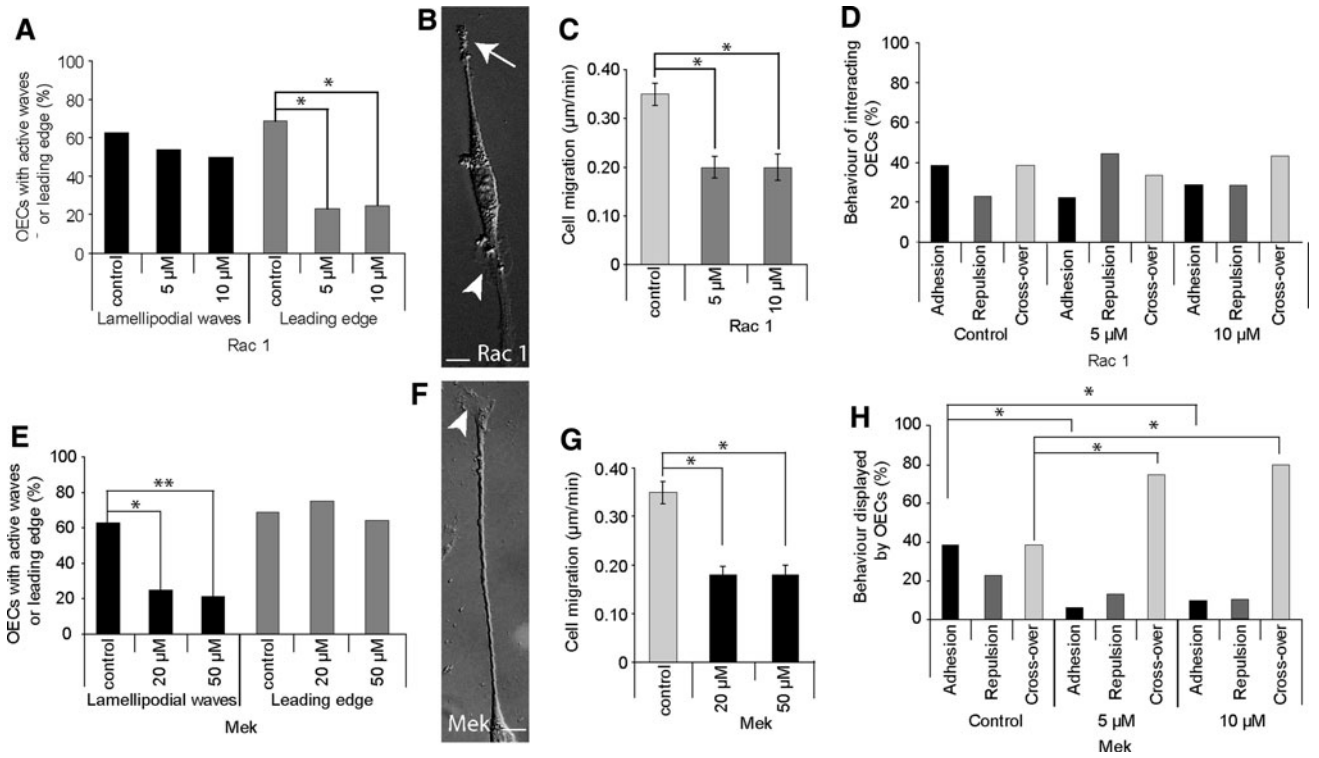

Fig. 6 Inhibition of wave activity via Mek alters central OEC behaviour. **a** Percentage of active lamellipodial waves and leading edge activity on isolated OECs following the addition of Rac 1 inhibitor (NSC23766) ($n = 15$–20); $p < 0.05$ chi-squared test, $^{*}p < 0.05$ post-hoc Fisher's exact test. **b** Addition of Rac 1 inhibitor reduced leading edge formation (*arrow*) while wave formation persisted (*arrowhead*); *scale bar* 10 μm. **c** Quantification of the migration rates of central OECs following the addition of Rac1 inhibitor ($n = 15$–20); $p < 0.05$ Kruskal-Wallis test, $^{*}p < 0.05$ post-hoc Dunn's multiple comparison test; *error bars* standard error of the mean. **d** Addition of Rac1 did not alter central OEC behaviour during cell–cell contact ($n = 7$–15). **e** Percentage of active lamellipodial waves and leading edge activity on isolated OECs following the addition of Mek inhibitor (ethanolate U0126) ($n = 15$–20); $p < 0.01$ chi-squared test, $^{*}p < 0.05$, $^{**}p < 0.001$ post-hoc Fisher's exact test. **f** Addition of Mek inhibitor reduced wave formation while leading edge activity persisted (*arrowhead*); *scale bar* 10 μm. **g** Quantification of the migration rates of central OECs following the addition of Mek inhibitor ($n = 16$–20); $p < 0.05$ Kruskal-Wallis test, $^{*}p < 0.05$ post-hoc Dunn's multiple comparison test; *error bars* standard error of the mean. **h** Following the addition of Mek inhibitor, OECs no longer respond to each other; crossover events become the predominant behaviour ($n = 7$–15); $p < 0.05$ chi-squared test, $^{*}p < 0.05$ post-hoc Fisher's exact test

with the findings in peripheral OECs, in rostral OECs inhibition of Rac1 by NSC23766 significantly reduced leading edge activity but did not significantly affect lamellipodial waves (Fig. 6a–b). In contrast, the response to Mek1 inhibition by ethanolate U0126 was the reverse with no significant effect on leading edge activity, but instead lamellipodial wave activity was significantly decreased (Fig. 6e–f). Rostral OEC migration was significantly decreased when the leading edge (Fig. 6c) or lamellipodial wave formation (Fig. 6g) was inhibited. These results suggest that both the leading edge and lamellipodial waves are integral in maintaining normal migration rates.

We next investigated whether specifically inhibiting lamellipodial waves would alter the responses to cell–cell contact. As stated above, rostral OECs continued to display a heterogeneous mix of behaviour during cell–cell contact (Figs. 2a–c, 4k) irrespective of the age of the donor tissue. When the leading edge activity was reduced by inhibition of Rac1, the resultant behaviour of interacting rostral OECs remained constant with an equal mix of adhesion, repulsion and crossover events (Fig. 6d). In contrast, when lamellipodial wave activity was reduced by inhibition of Mek1 at concentrations of both 5 μM and 10 μM there was a significant decrease in adhesion events and an increase in crossover behaviour (Fig. 6h). Thus, inhibition of lamellipodial waves resulted in over 80% of rostral OECs becoming nonresponsive to each other during cell–cell contact (Fig. 6h). These results suggest that lamellipodial waves are crucial cellular components in maintaining intrinsic behaviours during cell–cell contact.

Discussion

We report here for the first time that there are intrinsic fundamental differences in the cellular behaviour of OECs

from different anatomical locations of the olfactory bulb. We showed that central OECs are not a uniform population of cells, but instead they are a functionally heterogeneous population that exhibits a mix of responses including adhesion, repulsion and crossover during cell–cell interactions. These differences were reflected in OEC-axon assays where axons grown on central OECs were more dispersed than axons on peripheral OECs. We also showed that dynamic lamellipodial protrusions along the shaft of OECs mediate the cell–cell interactions as inhibition of lamellipodial waves altered the intrinsic behaviours of interacting OECs.

The differences in the responses to cell–cell interactions in OECs is consistent with their proposed roles in the various anatomical locations within the olfactory system. In mice, axons of olfactory sensory neurons leave the olfactory epithelium in fascicles that coalesce to form the olfactory nerve, with each fascicle being encased by OECs [33]. In the periphery, therefore, OECs migrate out and surround the primary olfactory axons to form tightly bundled fascicles. The in vitro assays demonstrated that peripheral OECs undergo cell–cell adhesion and contact-mediated migration consistent with their in vivo role. Later in development, the olfactory sensory axons and OECs reach and fuse with the telencephalon and then migrate into the presumptive NFL of the olfactory bulb [4, 9]. In the NFL, axons defasciculate from their intermixed bundles and sort out depending on the type of odorant receptor they express, and OECs are thought to contribute to the defasciculation and sorting process. Indeed, our assays of embryonic olfactory axons with peripheral or central OECs reflect these differences. When grown on peripheral OECs, the axons were typically closely associated with each other and resembled a fascicle formation, whereas when grown on OECs from the olfactory bulb the axons were more dispersed. OECs are known to differentially express axon guidance or adhesion molecules. For example, semaphorin 3A is expressed in the ventral NFL but is absent from regions where axons that express neuropilin-1 enter the NFL [21], the carbohydrate binding protein galectin-1 is widely expressed by OECs in the ventral/medial NFL, but is sparsely expressed in the dorsal/lateral NFL [22], and ephrin-B2 is strongly expressed in the periphery of the NFL during embryogenesis but becomes widespread throughout the NFL with increasing development [34]. Thus, the sorting of axons within the NFL probably involves the axons interacting with different subpopulations of OECs which themselves have to migrate to the appropriate regions. In the experiments described here we observed for the first time that central OECs undergoing cell–cell contact show a mix of responses in vitro: adhesion, repulsion or crossover, indicating that central OECs respond differentially to each other.

We further examined subpopulations of central OECs from the different anatomical locations within the olfactory bulb and found that these OECs did indeed respond differentially to cell–cell contact. The rostral NFL consists of prominent outer and inner NFLs. The oNFL is the region where axons defasciculate and sort out whereas the iNFL is the region where axons refasciculate and project to glomeruli [8]. The OECs in these layers have different antigenic profiles [8, 35] and are thought to play different roles in axon guidance. In addition, two subpopulations of OECs within the NFL as a whole have been identified using whole-cell voltage-clamp recordings with the differences being attributed to the gap-junction connectivity of the cells [36]. We analysed the OECs from the rostral NFL as a single culture of cells as it was not possible to dissect out the iNFL separate from the oNFL. However, the differing roles of OECs in these two layers of NFL were reflected in our in vitro assays with rostral OECs displaying a mix of adhesion, repulsion and crossover. It is possible that the differences in the responses to cell–cell contact could lead to the differential establishment of gap junctions which define two subpopulations of OECs [36]. Moreover, irrespective of the age of the tissue from which they were derived, rostral OECs consistently displayed these three different types of behaviour. This suggests that the rostral region of the NFL may be important in continually sorting incoming coalescent axon bundles from the peripheral nerve. In contrast, the NFL from the dorsal and caudal regions of the NFL is much more compact without a clear distinction between the inner and outer NFL. OECs derived from the caudal and dorsal NFL displayed a shift towards more adhesive responses that increased with developmental age. Axons that project to these regions of the NFL have already mostly been sorted in the rostral NFL. Thus, because there is less need for a complex sorting process in the dorsal and caudal NFL, these OECs are likely to be more involved in the maintenance (adhesion) of established pathways and are likely to have a reduced role in sorting. The behaviour of axons and their interactions with the different subpopulations of OECs will be examined in detail in future studies.

We have previously reported that peripheral OECs exhibit highly dynamic lamellipodia along their shafts and are important for initiating cell–cell interactions and mediating cell migration [13]. We have now shown that these highly motile plasma membrane protrusions also exist on central OEC shafts and are essential in regulating cell–cell interactions. In contrast to lamellipodial waves on peripheral OECs, which predominantly regulate adhesion [13], the lamellipodial waves on central OECs mediate a mix of adhesive, repulsive and crossover behaviours.

Consistent with previous reports [29] and similar to its effect on peripheral OECs [13], we have confirmed that

GDNF stimulates wave activity and migration of central OECs. This was confirmed by the finding that GDNF increased the activity and size of lamellipodial waves. Moreover, this behaviour was mediated through JNK and SRC kinases as recently reported for GDNF stimulation of OEC migration [29]. These results provide a clear link between wave activity and the migration rate of central OECs. We found, however, that GDNF does not alter intrinsic behaviours of central OECs associated with cell–cell contact.

While similar structures to that of lamellipodial waves have been reported on other cells types including Schwann cells [37] and fibroblasts [38], the role of lamellipodial waves on OECs is distinctly different. The role of radial lamellae on Schwann cells has been suggested to be associated with myelinating peripheral axons [37], whereas peripheral lamellae on fibroblasts are involved in regulating the direction of migration [38]. We predicted instead that lamellipodial waves on central OECs are a unique mechanism by which molecular/receptor complexes are presented to surrounding cells leading to the rapid identification of neighbouring cells. Lamellipodial wave formation was inhibited via the Mek pathway, which caused collapse of the waves, but the activity of the leading edge was maintained. Without active lamellipodial waves, central OECs ceased to respond to each other during cell–cell contact (Fig. 7a). Thus, lamellipodial waves act independently of the leading edge and are essential for OEC cell recognition and mediation of the response to cell–cell contact. Future work will determine the signalling molecules which are present on lamellipodial waves that are responsible for mediating OEC identification.

The effects of OECs on neural regeneration have been investigated in numerous studies. However, with regard to the source of the OECs, both peripheral and central OECs have been used [39]. To date central OECs used for transplantation therapies have often been acquired from the entire NFL of the olfactory bulb [40–44]. However, central OECs have been used in other studies without specifying the topographical locations from which they were obtained [45] or a more restricted population of central OECs, such as those from the rostral region of the olfactory bulb [46] or the ventral olfactory bulb [47], have been used. Peripheral OECs from the lamina propria have also been used [48], particularly as they have relevance to human trials [49]. The outcomes of these neural regeneration trials have been mixed, with the characteristics of the population of OECs being considered to be one of the sources of variation. It would therefore be of interest to determine how lamellipodial waves and the functional heterogeneity of central and peripheral OECs could be manipulated to improve therapeutic outcomes.

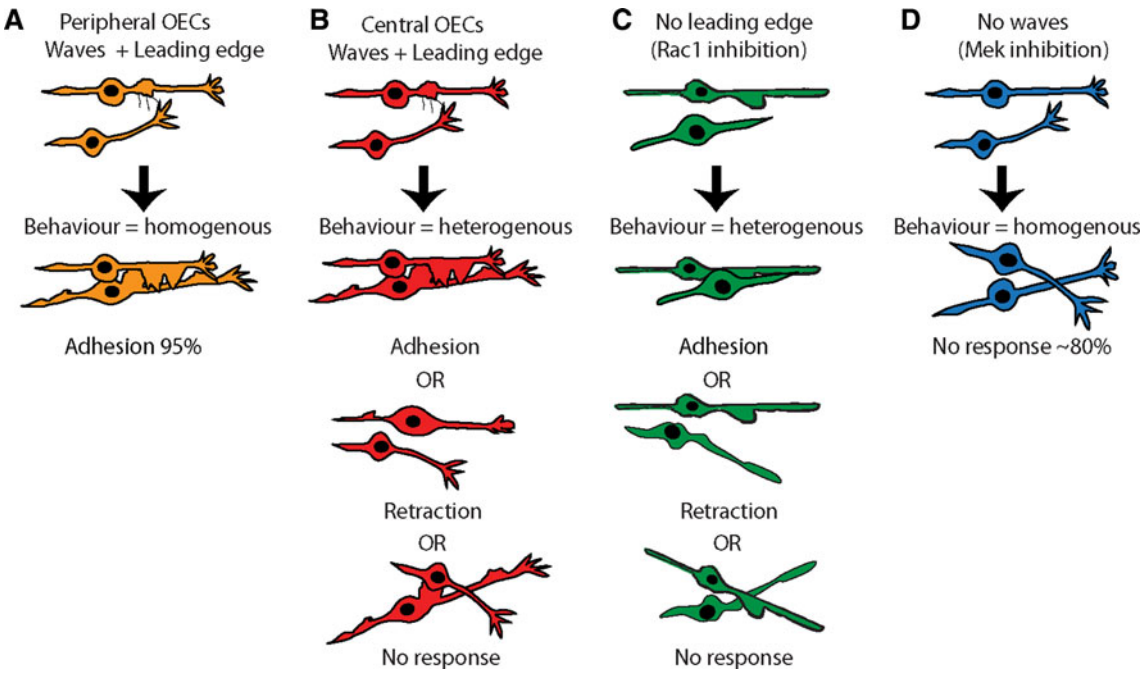

Fig. 7 Lamellipodial waves regulate central OEC behaviour during cell–cell contact. **a** During contact between peripheral OECs, the presence of lamellipodial waves and an active leading edge results predominantly in cell–cell adhesion. **b** During cell–cell contact between central OECs, there is a mix of adhesion, repulsion and crossover (no response) behaviours. **c** In the absence of the leading edge, the behaviour of interacting OECs is regulated by lamellipodial waves and remains heterogeneous in nature. **d** In the absence of lamellipodial waves, however, OECs do not respond to each other and the resultant behaviour following cell–cell interaction is predominantly crossover

In summary, OECs within the NFL of the olfactory bulb display intrinsically different patterns of behaviour during cell–cell contact which are dependent on their anatomical location within the NFL and the developmental age of the animal. Further, the behaviour of central OECs is dramatically different from the behaviour of peripheral OECs and their behaviours are consistent with their proposed roles in vivo. Importantly, the heterogeneity of responses by central OECs is mediated by lamellipodial waves. How these fundamental differences in intrinsic OEC properties affect axon regeneration will be the subject of future studies.

Acknowledgments This work was supported by a grant from the National Health and Medical Research Council to J.S. and B.K. (grant number 511006), by funding to the National Centre for Adult Stem Cell Research from the Australian Government Department of Health and Aging (A.M.S.) and by an Australian Postgraduate Award to L.W.

References

1. Chuah MI, Au C (1991) Olfactory Schwann cells are derived from precursor cells in the olfactory epithelium. J Neurosci Res 29:172–180
2. Doucette JR (1984) The glial cells in the nerve fiber layer of the rat olfactory bulb. Anat Rec 210:385–391
3. Farbman AI, Squinto LM (1985) Early development of olfactory receptor cell axons. Brain Res 351:205–213
4. Doucette JR (1989) Development of the nerve fiber layer in the olfactory bulb of mouse embryos. J Comp Neurol 285:514–527
5. Valverde F, Santacana M, Heredia M (1992) Formation of an olfactory glomerulus: morphological aspects of development and organization. Neuroscience 49:255–275
6. Doucette R (1990) Glial influences on axonal growth in the primary olfactory system. Glia 3:433–449
7. Mombaerts P, Wang F, Dulac C, Chao SK, Nemes A, Mendelsohn M, Edmondson J, Axel R (1996) Visualizing an olfactory sensory map. Cell 87:675–686
8. Au WW, Treloar HB, Greer CA (2002) Sublaminar organization of the mouse olfactory bulb nerve layer. J Comp Neurol 446:68–80
9. Treloar HB, Feinstein P, Mombaerts P, Greer CA (2002) Specificity of glomerular targeting by olfactory sensory axons. J Neurosci 22:2469–2477
10. St John JA, Key B (2001) Chemically and morphologically identifiable glomeruli in the rat olfactory bulb. J Comp Neurol 436:497–507
11. Royal SJ, Key B (1999) Development of P2 olfactory glomeruli in P2-internal ribosome entry site-tau-LacZ transgenic mice. J Neurosci 19:9856–9864
12. Potter SM, Zheng C, Koos DS, Feinstein P, Fraser SE, Mombaerts P (2001) Structure and emergence of specific olfactory glomeruli in the mouse. J Neurosci 21:9713–9723
13. Windus LC, Claxton C, Allen CL, Key B, St John JA (2007) Motile membrane protrusions regulate cell-cell adhesion and migration of olfactory ensheathing glia. Glia 55:1708–1719
14. Danciger E, Mettling C, Vidal M, Morris R, Margolis F (1989) Olfactory marker protein gene: its structure and olfactory neuron-specific expression in transgenic mice. Proc Natl Acad Sci USA 86:8565–8569
15. Margolis FL (1972) A brain protein unique to the olfactory bulb. Proc Natl Acad Sci USA 69:1221–1224
16. Astic L, Pellier-Monnin V, Godinot F (1998) Spatio-temporal patterns of ensheathing cell differentiation in the rat olfactory system during development. Neuroscience 84:295–307
17. Barnett SC, Hutchins AM, Noble M (1993) Purification of olfactory nerve ensheathing cells from the olfactory bulb. Dev Biol 155:337–350
18. Bailey MS, Puche AC, Shipley MT (1999) Development of the olfactory bulb: evidence for glia-neuron interactions in glomerular formation. J Comp Neurol 415:423–448
19. Gong Q, Bailey MS, Pixley SK, Ennis M, Liu W, Shipley MT (1994) Localization and regulation of low affinity nerve growth factor receptor expression in the rat olfactory system during development and regeneration. J Comp Neurol 344:336–348
20. Huang ZH, Wang Y, Cao L, Su ZD, Zhu YL, Chen YZ, Yuan XB, He C (2008) Migratory properties of cultured olfactory ensheathing cells by single-cell migration assay. Cell Res 18:479–490
21. Schwarting GA, Kostek C, Ahmad N, Dibble C, Pays L, Puschel AW (2000) Semaphorin 3A is required for guidance of olfactory axons in mice. J Neurosci 20:7691–7697
22. St John JA, Key B (1999) Expression of galectin-1 in the olfactory nerve pathway of rat. Brain Res Dev Brain Res 117:171–178
23. Storan MJ, Magnaldo T, Biol-N'Garagba MC, Zick Y, Key B (2004) Expression and putative role of lactoseries carbohydrates present on NCAM in the rat primary olfactory pathway. J Comp Neurol 475:289–302
24. Vincent AJ, Taylor JM, Choi-Lundberg DL, West AK, Chuah MI (2005) Genetic expression profile of olfactory ensheathing cells is distinct from that of Schwann cells and astrocytes. Glia 51:132–147
25. Au E, Roskams AJ (2003) Olfactory ensheathing cells of the lamina propria in vivo and in vitro. Glia 41:224–236
26. Jani HR, Raisman G (2004) Ensheathing cell cultures from the olfactory bulb and mucosa. Glia 47:130–137
27. Kumar R, Hayat S, Felts P, Bunting S, Wigley C (2005) Functional differences and interactions between phenotypic subpopulations of olfactory ensheathing cells in promoting CNS axonal regeneration. Glia 50:12–20
28. Vincent AJ, West AK, Chuah MI (2005) Morphological and functional plasticity of olfactory ensheathing cells. J Neurocytol 34:65–80
29. Cao L, Su Z, Zhou Q, Lv B, Liu X, Jiao L, Li Z, Zhu Y, Huang Z, Huang A, He C (2006) Glial cell line-derived neurotrophic factor promotes olfactory ensheathing cells migration. Glia 54:536–544
30. Bennett BL, Sasaki DT, Murray BW, O'Leary EC, Sakata ST, Xu W, Leisten JC, Motiwala A, Pierce S, Satoh Y, Bhagwat SS, Manning AM, Anderson DW (2001) SP600125, an anthrapyrazolone inhibitor of Jun N-terminal kinase. Proc Natl Acad Sci USA 98:13681–13686
31. Hanke JH, Gardner JP, Dow RL, Changelian PS, Brissette WH, Weringer EJ, Pollok BA, Connelly PA (1996) Discovery of a novel, potent, and Src family-selective tyrosine kinase inhibitor. Study of Lck- and FynT-dependent T cell activation. J Biol Chem 271:695–701
32. Lipson AC, Widenfalk J, Lindqvist E, Ebendal T, Olson L (2003) Neurotrophic properties of olfactory ensheathing glia. Exp Neurol 180:167–171
33. Whitesides JG 3rd, LaMantia AS (1996) Differential adhesion and the initial assembly of the mammalian olfactory nerve. J Comp Neurol 373:240–254
34. St John JA, Key B (2001) EphB2 and two of its ligands have dynamic protein expression patterns in the developing olfactory system. Brain Res Dev Brain Res 126:43–56

35. Franceschini I, Barnett S (1996) Low-affinity NGF-receptor and E-N-CAM expression define two types of olfactory nerve ensheathing cells that share a common lineage. Dev Biol 173:327–343
36. Rela L, Bordey A, Greer CA (2009) Olfactory ensheathing cell membrane properties are shaped by connectivity. Glia doi:10.1002/glia.20953
37. Nodari A, Zambroni D, Quattrini A, Court FA, D'Urso A, Recchia A, Tybulewicz VL, Wrabetz L, Feltri ML (2007) Beta1 integrin activates Rac1 in Schwann cells to generate radial lamellae during axonal sorting and myelination. J Cell Biol 177:1063–1075
38. Pankov R, Endo Y, Even-Ram S, Araki M, Clark K, Cukierman E, Matsumoto K, Yamada KM (2005) A Rac switch regulates random versus directionally persistent cell migration. J Cell Biol 170:793–802
39. Richter MW, Roskams AJ (2008) Olfactory ensheathing cell transplantation following spinal cord injury: hype or hope? Exp Neurol 209:353–367
40. Li Y, Field PM, Raisman G (1997) Repair of adult rat corticospinal tract by transplants of olfactory ensheathing cells. Science 277:2000–2002
41. Lopez-Vales R, Fores J, Navarro X, Verdu E (2006) Olfactory ensheathing glia graft in combination with FK506 administration promote repair after spinal cord injury. Neurobiol Dis 24:443–454
42. Lopez-Vales R, Fores J, Verdu E, Navarro X (2006) Acute and delayed transplantation of olfactory ensheathing cells promote partial recovery after complete transection of the spinal cord. Neurobiol Dis 21:57–68
43. Ramon-Cueto A, Cordero MI, Santos-Benito FF, Avila J (2000) Functional recovery of paraplegic rats and motor axon regeneration in their spinal cords by olfactory ensheathing glia. Neuron 25:425–435
44. Ramon-Cueto A, Plant GW, Avila J, Bunge MB (1998) Long-distance axonal regeneration in the transected adult rat spinal cord is promoted by olfactory ensheathing glia transplants. J Neurosci 18:3803–3815
45. Teng X, Nagata I, Li HP, Kimura-Kuroda J, Sango K, Kawamura K, Raisman G, Kawano H (2008) Regeneration of nigrostriatal dopaminergic axons after transplantation of olfactory ensheathing cells and fibroblasts prevents fibrotic scar formation at the lesion site. J Neurosci Res 86:3140–3150
46. Lankford KL, Sasaki M, Radtke C, Kocsis JD (2008) Olfactory ensheathing cells exhibit unique migratory, phagocytic, and myelinating properties in the X-irradiated spinal cord not shared by Schwann cells. Glia 56:1664–1678
47. Guest JD, Herrera L, Margitich I, Oliveria M, Marcillo A, Casas CE (2008) Xenografts of expanded primate olfactory ensheathing glia support transient behavioral recovery that is independent of serotonergic or corticospinal axonal regeneration in nude rats following spinal cord transection. Exp Neurol 212:261–274
48. Ramer LM, Au E, Richter MW, Liu J, Tetzlaff W, Roskams AJ (2004) Peripheral olfactory ensheathing cells reduce scar and cavity formation and promote regeneration after spinal cord injury. J Comp Neurol 473:1–15
49. Mackay-Sim A, Feron F, Cochrane J, Bassingthwaighte L, Bayliss C, Davies W, Fronek P, Gray C, Kerr G, Licina P, Nowitzke A, Perry C, Silburn PA, Urquhart S, Geraghty T (2008) Autologous olfactory ensheathing cell transplantation in human paraplegia: a 3-year clinical trial. Brain 131:2376–2386